

Original Article

Therapeutic effects of adipose derived fresh stromal vascular fraction-containing stem cells versus cultured adipose derived mesenchymal stem cells on rescuing heart function in rat after acute myocardial infarction

Jiunn-Jye Sheu^{1,6}, Mel S Lee², Christopher Glenn Wallace⁷, Kuan-Hung Chen³, Pei-Hsun Sung^{4,5}, Sarah Chua^{4,6}, Fan-Yen Lee^{1,5,6,8}, Sheng-Ying Chung⁴, Yi-Ling Chen^{4,6}, Yi-Chen Li⁴, Hon-Kan Yip^{4,5,6,9,10}

¹Division of Thoracic and Cardiovascular Surgery, Department of Surgery, ²Department of Orthopedics, ³Department of Anesthesiology, ⁴Division of Cardiology, Department of Internal Medicine, Kaohsiung Chang Gung Memorial Hospital and Chang Gung University College of Medicine, Kaohsiung 83301, Taiwan; ⁵Center for Shockwave Medicine and Tissue Engineering, ⁶Institute for Translational Research in Biomedicine, Kaohsiung Chang Gung Memorial Hospital, Kaohsiung 83301, Taiwan; ⁷Department of Plastic Surgery, University Hospital of South Manchester, Manchester, UK; ⁸Division of Cardiovascular Surgery, Department of Surgery, Tri-Service General Hospital, National Defense Medical Center, Taipei 11490, Taiwan; ⁹Department of Medical Research, China Medical University Hospital, China Medical University, Taichung 40402, Taiwan; ¹⁰Department of Nursing, Asia University, Taichung 41354, Taiwan

Received August 12, 2018; Accepted December 23, 2018; Epub January 15, 2019; Published January 30, 2019

Abstract: We tested the hypothesis that adipose-derived fresh stromal vascular fraction (SVF) is non-inferior to conventional adipose-derived mesenchymal stem cell (ADMSC) therapy for improving left-ventricular ejection fraction (LVEF) in rat after acute myocardial infarction (AMI). Male-adult SD rats (n = 48) were categorized into group 1 (sham control), AMI, AMI + ADMSCs (1.2×10^6 cells) and AMI + SVF (1.2×10^6 cells). Flow cytometric and qPCR analyses showed that the expressions of surface biomarkers for endothelial progenitor cells, and cardiac-stem cells were significantly higher in the SVF population than in the ADMSC population, whereas MSCs showed a reversed pattern between these two groups (all $P < 0.001$). By day-42 after AMI, LVEF was highest in SC, lowest in AMI, and significantly higher in AMI + SVF than in AMI + ADMSCs ($P < 0.0001$). Protein expression indicating angiogenesis, anti-inflammatory/anti-apoptotic, mitochondrial/bioenergy-integrity and antifibrotic biomarkers showed an identical pattern, whereas protein expressions for inflammatory, apoptotic and pressure-overload/heart failure biomarkers exhibited an opposite pattern to LVEF among the four groups (all $P < 0.001$). Histopathology displayed that LV infarction/fibrotic area/collagen-deposition areas, cellular expressions of DNA-damage, and inflammatory biomarkers exhibited an opposite pattern, whereas cellular expressions of endothelial/gap-junction biomarkers showed an identical pattern to LVEF among the four groups (all $P < 0.0001$). Cellular expression of angiogenesis biomarkers significantly and progressively increased from groups 1 to 4 (all $P < 0.0001$). In conclusion, SVF may be better than ADMSC at improving LVEF in rat after AMI.

Keywords: Acute myocardial infarction, fresh stromal-vascular fraction containing stem cells, adipose-derived mesenchymal stem cells, heart function

Introduction

In-hospital mortality following acute myocardial infarction (AMI), especially if complicated by cardiogenic shock, remains unacceptably high even despite primary percutaneous coronary intervention (PCI) [1-5]. Readmission rates for heart failure and post-discharge mortality are also high in this population [6-10]. Novel, safe

and effective treatments that can improve outcomes following AMI therefore remain of utmost importance.

Abundant data have shown that cell therapy improved ischemia-related organ dysfunction in various cardiovascular diseases [11-14]. Both experimental and clinical trials have further demonstrated that endothelial progenitor cell

SVF and ADMSC on rescuing heart function in rat after acute myocardial infarction

(EPC)/mesenchymal stem cell (MSC) therapy also effectively improved heart function, reduced congestive heart failure, and inhibited left ventricle (LV) remodeling following AMI [11-13, 15, 16]. Previous studies [17-19] showed that, compared with bone marrow-derived MSCs, adipose-derived (AD) MSCs have distinct advantages of being abundant, easy to obtain with minimal invasiveness, readily cultured to a sufficient number for autologous transplantation, and having higher anti-inflammatory and immunomodulatory capacity. However, these MSCs need cell culture and expansion for at least 10-14 days to produce enough quantities for cell therapy to proceed. These procedures may therefore be viewed as impractical for daily clinical practice when prompt application of ADMSCs would be necessary to treat ischemia-related organ dysfunction. Accordingly, a therapeutic modality that is safe and has comparable effects to AMDSC therapy but can be prepared urgently in the setting of ischemia-related organ dysfunction is of importance.

Recently, it has been shown that a simple and quick preparation (i.e., without cell culture) of adipose-derived fresh stromal vascular fraction (SVF) containing primitive stem cells can be utilized immediately with promising results in accelerating wound healing through angiogenesis and anti-inflammation [20]. It was revealed that the adipose-derived fresh SVF contained heterogeneous populations of undifferentiated, mononucleated elements based on cell surface antigens within those multipotent tissues [21]. This MSC-derived uncultured/heterogeneous SVF has thus emerged as an easy and safe way to treat various diseases [21-23]. However, there has seldom been mention [24] of the impact of SVF on LV function following AMI and only with uncertain results. We sought to determine whether adipose-derived fresh SVF therapy might also be effective at restoring LV function and inhibiting LV remodeling after AMI.

Materials and methods

Ethics

All animal procedures were approved by the Institute of Animal Care and Use Committee at Kaohsiung Chang Gung Memorial Hospital (Affidavit of Approval of Animal Use Protocol No.

2015061504) and performed in accordance with the Guide for the Care and Use of Laboratory Animals.

Animals were housed in an Association for Assessment and Accreditation of Laboratory Animal Care International (AAALAC; Frederick, MD, USA)-approved animal facility in our hospital with controlled temperature and light cycles (24°C and 12/12 light cycle).

Animal grouping

Pathogen-free, adult male Sprague Dawley rats ($n = 48$) weighing 325-350 g (Charles River Technology, BioLASCO, Taiwan) were categorized into four groups: group 1 [sham control; chest wall opened and the left anterior descending artery (LAD) was identified], group 2 [acute myocardial infarction (AMI); induced by ligation of LAD], group 3 [AMI + ADMSC (1.2×10^6)/direct implantation of cells into the infarct area 2 h after AMI induction], and group 4 [AMI + adipose-derived fresh SVF (1.2×10^6)/direct implantation of SVF into the infarct area 2 h after AMI induction]. The stem cell doses utilized in the present study were based on our previous reports [25, 26].

In our study, six animals in each group were utilized for cross-section of heart for identifications of infarction, fibrotic and collagen-deposition areas. Additional six animals in each group were utilized for molecular-cellular levels of the studies.

Animal model of AMI

The procedure and protocol of AMI induction were based on our recent reports [25, 26]. All animals were anesthetized (inhalational 2.0% isoflurane) supine on a warming pad at 37°C and, under sterile conditions, the heart was exposed via a left thoracotomy. Sham-operated rats (SC) received thoracotomy alone, while AMI in other groups was induced by left coronary artery ligation 3 mm distal to the margin of the left atrium with 7-0 prolene. Regional myocardial ischemia was verified by observing a rapid color change from pinkish to dull reddish over the anterior surface of the LV and rapid development of akinesia and dilatation in the ischemic region. After the procedure, the thoracotomy wound was closed, and the animals recovered from anaesthesia in a portable ani-

SVF and ADMSC on rescuing heart function in rat after acute myocardial infarction

mal intensive care unit (ThermoCare®) for 24 hours.

Functional assessment by echocardiography

Transthoracic echocardiography (Vevo 2100, Visualsonics, Toronto, Ontario, Canada) was performed in animals from each group prior to and at day 60 after doxorubicin treatment by a veterinary cardiologist blinded to the experimental design. M-mode standard two-dimensional (2D) left parasternal long axis echocardiographic examination was conducted. Left ventricular internal dimensions [i.e., left ventricular end-systolic diameter (LVESd) and left ventricular end-diastolic diameter (LVEDd)] were measured at mitral valve and papillary levels of the left ventricle, as per the American Society of Echocardiography (Morrisville, NC) leading-edge methodology, using at least three consecutive cardiac cycles. Left ventricular ejection fraction (LVEF) was calculated as follows: $LVEF (\%) = [(LVEDd^3 - LVESd^3) / LVEDd^3] \times 100\%$.

Procedure and protocol for isolation of adipose-derived fresh SVF

The procedure and protocol for preparing SVF was based on a previous report [27]. The rats in group 4 were anesthetized with inhalational isoflurane 3 h prior to AMI induction. Both inguinal regions of the rats were clipped and prepared with 10% povidone iodine, the inguinal fat pads were removed, and $1 \times 1 \times 1$ cm (1 cm^3) of adipose tissue excised from each. The incisions were closed with 3/0 silk sutures. We pooled all the cells from the same rats to make a master batch of SVF. The excised adipose tissues were washed extensively by phosphate buffer solution (PBS, Sigma1) to remove the contaminating debris and red blood cells and then minced with fine tissue scissors. The fragmented tissues were incubated with 0.1% collagenase (collagenase from *Clostridium histolyticum* C0130, Sigma1) and kept in a slow shaking water bath at 37°C for 60 min. Thereafter, collagenase was removed by diluting the samples with PBS. The cell suspension was centrifuged twice at 1300 rpm (260 G) for 5 min. The supernatant containing mature adipocytes was removed. The precipitate was passed through 100 μm mesh filter and used as SVF. Viable cells were measured by adding trypan blue to SVF and counting them with

Thoma slide. There were approximately 4×10^6 /ml viable cells.

Procedure and protocol for isolating and culturing ADMSCs

The procedure and protocol for ADMSC isolation and culture have previously been described [28-30]. Briefly, adipose tissue surrounding the epididymis was dissected, excised and prepared. For purification, the harvested cells were cultured in Dulbecco's modified Eagle's medium (DMEM)-low glucose medium containing 10% FBS for 14 days. By this time plentiful ADMSCs were obtained in the culture plate and were collected to treat AIS animals. Surface markers for ADMSCs were identified by flow cytometric analyses as previously reported [28-30].

The procedure and protocol for qPCR

Total RNA was isolated using the TRIzol® RNA isolation reagents (Invitrogen), and 1 μg of total RNA was subjected to reverse transcription with Transcriptor First Strand cDNA Synthesis Kit (Roche). For the quantitative real-time RT-PCR, cDNA synthesis was performed using the Maxima Probe/ROX qPCR Master Mix (ThermoFisher) containing ROX passive reference dye. Real-time fluorescence monitoring and the melting curve analysis were performed with LightCycler (Roche) according to the manufacturer's recommendations. The relative transcript amount of the target gene, calculated using standard curves of serial RNA dilutions, was normalized to that of glyceraldehyde-3-phosphate dehydrogenase (GAPDH) of the same RNA.

Western blot analysis

As previously reported [28-31], equal amounts (50 μg) of protein extracts were loaded and separated by SDS-PAGE using acrylamide gradients. After electrophoresis, the separated proteins were transferred electrophoretically to a polyvinylidene difluoride (PVDF) membrane (Amersham Biosciences). Nonspecific sites were blocked by incubation of the membrane in blocking buffer [5% nonfat dry milk in T-TBS (TBS containing 0.05% Tween 20)] overnight. The membranes were incubated with the indicated primary antibodies [mitochondrial (mit)-Bax (1:1000, Abcam), cleaved caspase 3

SVF and ADMSC on rescuing heart function in rat after acute myocardial infarction

Table 1. Comparison of flow cytometric results between adipose-derived fresh SVF- and cultured ADMSC-derived stem cell surface markers (n = 6)

Surface markers	SVF*	ADMSC*	p-value
CD73	51.82 ± 2.34	96.85 ± 0.39	< 0.0001
CD90	38.78 ± 3.58	86.05 ± 5.25	< 0.0001
CD44	72.70 ± 4.29	96.28 ± 1.90	0.0008
CD271	10.97 ± 1.46	20.45 ± 1.23	0.0003
CD29	89.80 ± 3.58	99.78 ± 0.03	0.0192
CD105	34.78 ± 1.18	30.10 ± 1.37	0.0137
CD34	8.25 ± 1.46	4.53 ± 0.88	0.0298
CD133	3.23 ± 0.49	1.18 ± 0.32	0.0035
CXCR4	0.33 ± 0.02	0.17 ± 0.04	0.0251
KDR	0.95 ± 0.06	0.28 ± 0.03	< 0.0001
CD31	21.07 ± 2.43	1.30 ± 0.15	0.0002
C-kit	5.68 ± 0.54	2.42 ± 0.62	0.0013
Sca-1	1.65 ± 0.23	0.67 ± 0.28	0.0112
CD45	22.44 ± 2.70	4.37 ± 0.85	0.0004

Data are expressed as mean ± SD. *, SVF indicated adipose-derived fresh stromal vascular fraction (SVF); ADMSC indicated cultured adipose-derive mesenchymal stem cell (ADMSC).

(c-Csp3) (1:1000, Cell Signaling), cleaved poly (ADP-ribose) polymerase (PARP) (1:1000, Cell Signaling), Bcl-2 (1:200, Abcam), phosphorylated (p)-Smad3 (1:1000, Cell Signaling), p-Smad1/5 (1:1000, Cell Signaling), bone morphogenetic protein (BMP) 2 (1:5000, Abcam) transforming growth factor (TGF)- β (1:500, Abcam), interleukin (IL)-1 β (1:1000, Cell Signaling), matrix metalloproteinase (MMP)-9 (1:3000, Abcam), IL-10 (1:5000, Abcam), tumor necrosis factor (TNF)- α (1:1000, Cell Signaling), nuclear factor (NF)- κ B (1:600, Abcam), CXCR4 (1:1000, Abcam), stromal cell-derived factor (SDF)-1 α (1:1000, Cell Signaling), endothelial nitric oxide synthase (eNOS) (1:1000, Abcam), vascular endothelial cell growth factor (VEGF) (1:1000, Abcam), CD31 (1:1000, Cell Signaling), von Willebrand factor (vWF) (1:1000, Abcam), brain natriuretic peptide (BNP) (1:600, Abcam), myosin heavy chain (MHC)- α (1:300, Santa Cruz), MHC- β (1:1000, Santa Cruz), mitochondrial cytochrome C (mit-Cyto C) (1:2000, BD Biosciences), cytosolic cytochrome C (cyt-Cyto C) (1:2000, BD Biosciences) and actin (1:10000, Chemicon)] for 1 hour at room temperature. Horseradish peroxidase-conjugated anti-rabbit immunoglobulin IgG (1:2000, Cell Signaling) was used as a

secondary antibody for one-hour incubation at room temperature. The washing procedure was repeated eight times within one hour. Immunoreactive bands were visualized by enhanced chemiluminescence (ECL; Amersham Biosciences) and exposed to Biomax L film (Kodak). For purposes of quantification, ECL signals were digitized using Labwork software (UVP).

Immunohistochemical and immunofluorescent studies

The procedures and protocols for immunohistochemical (IHC) and immunofluorescent (IF) examinations were based on previous studies [31-33]. Briefly, for IHC staining, rehydrated paraffin sections were first treated with 3% H₂O₂ for 30 minutes and incubated with Immuno-Block reagent (BioSB) for 30 minutes at room temperature. Sections were then incubated with primary antibodies specifically against CD14 (1:300, Bio SS) at 4°C overnight. Irrelevant antibody (p53 [1:500, Abcam] and mouse control IgG [Abcam]) provided control in the current study. IF staining was performed for the examinations of Sca-1 (1:300, BioLegend), C-kit (1:300, Santa Cruz), CD14 (1:50, Santa Cruz), CD31 (1:100, Serotec), vWF (1:200, Millipore), VEGF (1:400, Abcam), SDF-1 α (1:100, Santa Cruz), CXCR4 (1:200, Bioss), connexin43 (Cx43) (1:200, Millipore), γ -H2AX (1:500, Abcam) and CD68 (1:100, Abcam) using respective primary antibody with irrelevant antibodies being used as controls. Three sections of kidney specimens were analyzed in each rat. For quantification, three randomly selected HPFs (\times 200 or 400 \times for IHC and IF studies) were analyzed in each section. The mean number per HPF for each animal was then determined by summation of all numbers divided by 9.

Vessel density and arterial muscularization in LV infarct area

The procedure and protocol were based on our previous report [32]. IHC staining of small blood vessels was performed with α -SMA (1:400) as primary antibody at room temperature for 1 hour, followed by washing with PBS thrice. Ten minutes after the addition of anti-mouse-HRP conjugated secondary antibody, the tissue sections were washed with PBS thrice. Then 3,3' diaminobenzidine (DAB) (0.7 gm/tablet) (Sigma)

SVF and ADMSC on rescuing heart function in rat after acute myocardial infarction

Table 2. Time courses of echocardiographic findings in animals after acute myocardial infarction

Variables	SC	AMI	AMI + ADMSC	AMI + SVF	p-value*
At day 14					
LVEDd (mm)	8.02 ± 0.19	8.14 ± 0.40	8.15 ± 0.12	8.13 ± 0.15	0.554
LVESd (mm)	4.59 ± 0.23 ^a	5.82 ± 0.27 ^b	5.28 ± 0.16 ^c	5.14 ± 0.15 ^c	< 0.0001
LVEF (%)	73.45 ± 2.62 ^a	52.63 ± 2.39 ^b	61.52 ± 3.52 ^c	63.51 ± 3.01 ^c	< 0.0001
At day 42					
LVEDd (mm)	8.11 ± 0.28 ^a	9.26 ± 0.25 ^b	9.28 ± 0.17 ^b	8.38 ± 0.33 ^a	< 0.0001
LVESd (mm)	4.64 ± 0.31 ^a	6.28 ± 0.25 ^b	5.73 ± 0.18 ^c	5.03 ± 0.20 ^d	< 0.0001
LVEF (%)	73.43 ± 2.71 ^a	54.61 ± 1.42 ^b	64.93 ± 1.33 ^c	68.72 ± 0.28 ^d	< 0.0001

Data are expressed as mean ± SD. *The distribution of these parameters was nonparametric, statistical analysis was appropriately performed by Kruskal-Wallis test followed by post hoc multiple-comparison analysis. Letters (a, b, c) indicate significant difference exists between two different groups (^aindicates P < 0.001, ^bindicates P < 0.001, ^cindicates P = 0.003).

was added, followed by washing with PBS thrice after one minute. Finally, hematoxylin was added as a counter-stain for nuclei, followed by washing twice with PBS after one minute. Three heart sections were analyzed in each rat. For quantification, three randomly selected HPFs (200 ×) were analyzed in each section. The mean number per HPF for each animal was then determined by summation of all numbers divided by 9.

Muscularization of the arterial medial layer (an index of vascular remodeling) in the LV infarct area was defined as a mean thickness of vessel wall greater than 50% of the lumen diameter in a vessel of diameter > 50 μm. Arteriolar diameter and wall thickness were measured using Image-J software (NIH, Maryland, USA).

Histological studies of fibrosis, collagen deposition and infarct areas

The procedure and protocol for histological studies of fibrosis, collagen-deposition and infarct areas have been described in our previous report [32]. Masson's trichrome and Sirius red staining were used to study fibrosis and collagen deposition in LV myocardium and H.E. stain to identify the infarct area. Three 4 μm thick serial sections of LV myocardium were prepared by Cryostat (Leica CM3050S). The integrated area (μm²) of fibrosis in each section was calculated using Image Tool 3 (IT3) software (University of Texas, Health Science Center, San Antonio, UTHSCSA; Image Tool for Windows, Version 3.0, USA). Three sections were quantified for each animal and three randomly selected HPFs (100 ×) were analyzed in each section. The number of pixels in each fibrotic area per HPF were determined, and

then summated from the three HPFs. The procedure was repeated in two other sections for each animal. The mean pixel number per HPF for each animal was then determined by summing all pixel numbers and dividing by 9. The mean integrated area (μm²) of fibrosis and collagen deposition in LV myocardium per HPF was obtained using a conversion factor of 19.24 (1 μm² represented 19.24 pixels).

Statistical analysis

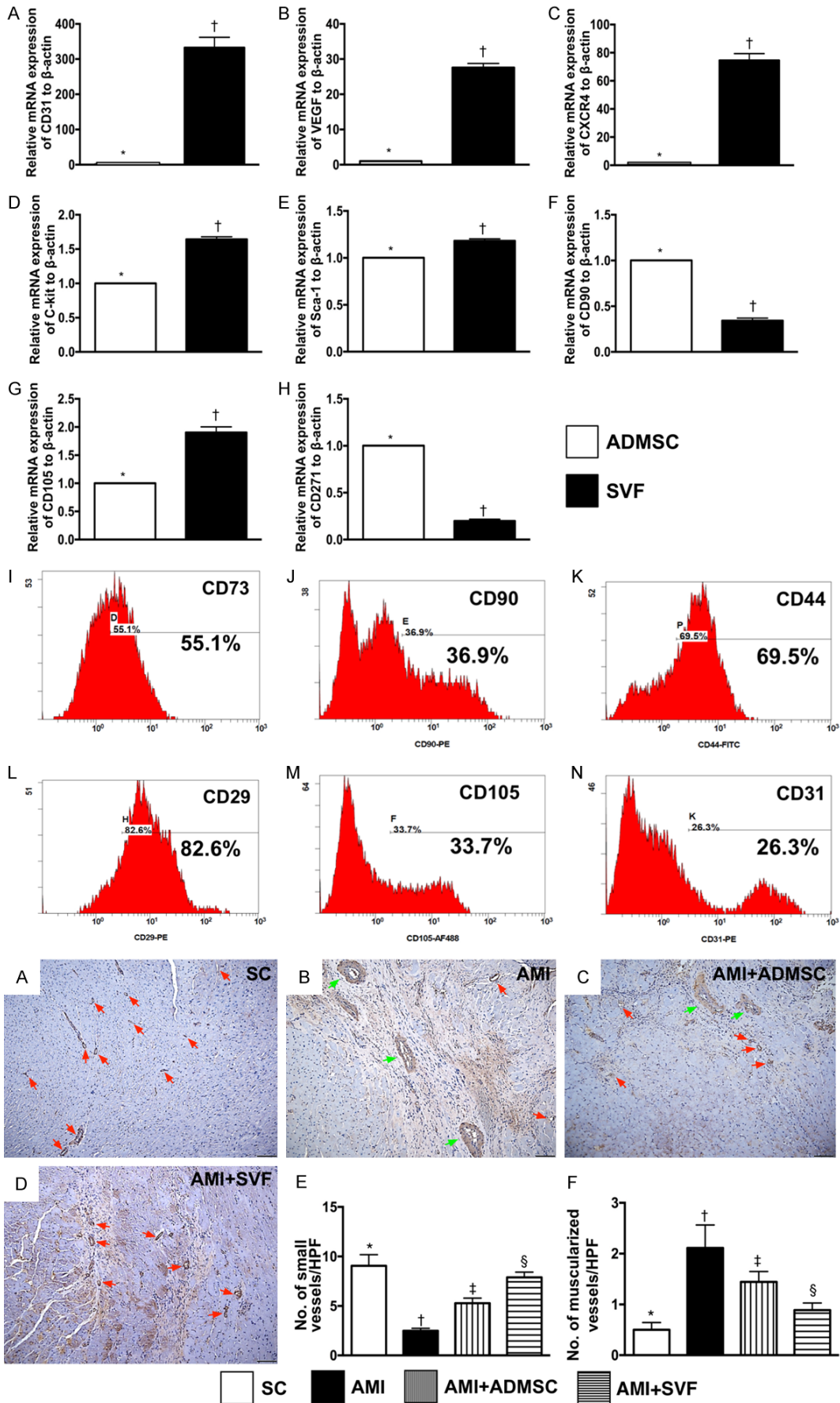
Quantitative data are expressed as means ± SD. For **Tables 1** and **2**, continuous variables among different groups were analyzed with Kruskal-Wallis test according to nonparametric statistics. Additionally, for **Figures 1** and **9**, all statistical analyses were performed by one-way ANOVA, followed by Bonferroni multiple comparison post hoc test (n = 6 for each group). Statistical analysis was performed by using SPSS statistical software for Windows version 17 (SPSS for Windows, version 17; SPSS, IL, U.S.A.). A P-value of less than 0.05 was considered statistically significant.

Results

Comparison of flow cytometric results between adipose-derived fresh SVF and cultured ADMSC (Table 1)

Flow cytometry showed that the MSC surface markers (CD73, CD90, CD44, CD217) were significantly lower in the SVF group than in the ADMSC group. On the other hand, the EPC surface markers (CD105, CD34, CD133, CXCR4, KDR), endothelial cell (EC) marker (CD31) and cardiac stem cell markers (C-kit, Sca-1) as well as leukocyte/ hematopoietic cell (CD45) maker

SVF and ADMSC on rescuing heart function in rat after acute myocardial infarction



SVF and ADMSC on rescuing heart function in rat after acute myocardial infarction

Figure 1. Gene expressions of EPCs, ECs, MSC and cardiac stem cells in SVF and ADMSC and illustrating the higher subpopulation of stem cells in SVF, and small vessel density and muscularization in LV infarct area by day 42 after AMI induction. Upper panel: A. mRNA expressions of CD31, * vs. †, P < 0.001. B. mRNA expressions of vascular endothelial growth factor (VEGF), * vs. †, P < 0.001. C. mRNA expressions of CXCR4, * vs. †, P < 0.001. D. mRNA expressions of C-kit, * vs. †, P < 0.001. E. mRNA expressions of Sca-1, * vs. †, p<0.001. F. mRNA expressions of CD90, * vs. †, P < 0.001. G. mRNA expressions of CD105, * vs. †, P < 0.001. H. mRNA expressions of CD217, * vs. †, P < 0.001. I-N. Illustrating the higher subpopulations of stem cells in SVF. EPC = endothelial progenitor cell; EC = endothelial cell; MSC = mesenchymal stem cell; SVF = stromal vascular fraction; ADMSC = adipose-derived mesenchymal stem cell. n = 6 for each group. Lower panel: A-D. Illustrating the microscopic finding (100 ×) of α -smooth muscle actin (SMA) for identification of small vessels (< 25 μ M) (red arrows). E. Analytical result of number of small vessels, * vs. other group with different symbols (†, ‡, §), P < 0.0001. F. Analytical result of number of muscularization (red arrows), * vs. other group with different symbols (†, ‡, §), P < 0.0001. Symbols (*, †, ‡, §) indicate significance (at 0.05 level). SC = sham control; AMI = acute myocardial infarction; ADMSC = adipose-derived mesenchymal stem cell; SVF = stromal vascular fraction.

were significantly higher in the SVF group than in the ADMSC group.

Time courses of transthoracic echocardiographic findings prior to after acute myocardial infarction in four groups of animals (Table 2)

By day 14 after AMI, the left ventricular end-diastolic diameter (LVEDd) was also did not differ among the SC (i.e., sham-control), AMI, AMI + ADMSC and AMI + SVF. However, the left ventricular end-systolic diameter (LVESd) was significantly higher in AMI than in groups SC, AMI + ADMSC and AMI + SVF, and significantly higher in AMI + ADMSC and AMI + SVF than in SC, but it showed no difference between AMI + ADMSC and AMI + SVF. Furthermore, the left ventricular ejection fraction (LVEF) exhibited an opposite pattern of LVESd among the four groups.

By day 42 after AMI induction, the LVEDd was significantly higher in AMI and AMI + ADMSC than in SC and AMI + SVF, and significantly higher in AMI + SVF than in SC, but it showed no difference between AMI and AMI + ADMSC. Additionally, the LVESd was highest in AMI, lowest in SC, and significantly higher in AMI + ADMSC than in AMI + SVF. On the other hand, the LVEF displayed an opposite pattern of LVESd among the four groups. These findings suggested that ADMSC-SVF therapy improved left ventricular (LV) function and inhibited LV remodeling in animals after AMI induction.

qPCR measurement of the gene expressions of EPCs, ECs, MSC and cardiac stem cells in SVF and ADMSC, and assessment of numbers of small vessel and muscularization in LV infarct area by day 42 after AMI induction (Figure 1)

The mRNA expressions of CD31 and VEGF, two EC biomarkers, were significantly higher in SVF

group than in ADMSC group. The mRNA expressions of CXCR4 and KDR, in indicator of EPCs, exhibited an identical pattern of EC between the two groups. The mRNA expressions of C-kit and Sca-1, two indicators of cardiac stem cells, displayed an identical pattern to EC between the two groups. The mRNA expressions of CD90, CD105, CD217, CD29, four indicators of MSCs, displayed an opposite pattern to EC between two groups.

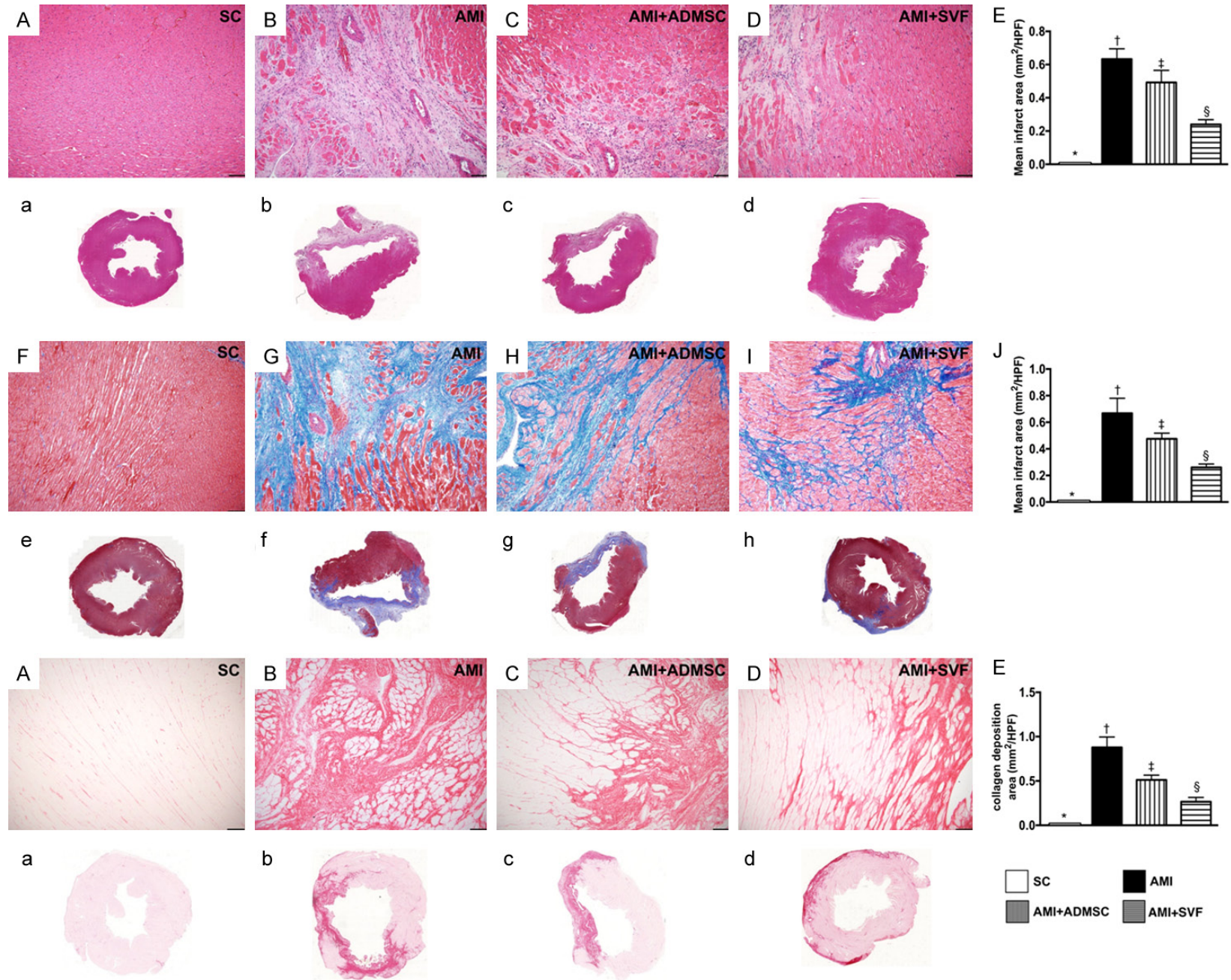
The number of small vessels (< 25 μ M) in the infarct area was highest in SC, lowest in AMI, and significantly higher in AMI + SVF than in AMI + ADMSC. Arteriolar muscularization in the infarct area expressed an opposite pattern (to the number of small vessels) among the four groups.

Microscopic findings of infarct area, fibrotic area, collagen deposition area and the cellular expression of heart failure biomarker in LV myocardium by day 42 after AMI induction (Figure 2)

Hematoxylin and eosin (H&E) staining showed that the infarct areas were largest in AMI, smallest in SC, and significantly larger in AMI + ADMSC than in AMI + SVF. Masson's trichrome stain demonstrated that the fibrotic area showed an identical pattern to the infarct area among the four groups.

Additionally, IHC microscopy with Sirius red stain displayed that the collagen deposition area, an indicator of increased cardiomyocyte death and fibroblast activity, was largest in AMI, smallest in SC, and significantly larger in AMI + ADMSC than in AMI + SVF. Furthermore, the number of BNP+ cells, an indicator of pressure overload/heart failure, expressed an identical pattern to collagen deposition area among the four groups.

SVF and ADMSC on rescuing heart function in rat after acute myocardial infarction



SVF and ADMSC on rescuing heart function in rat after acute myocardial infarction

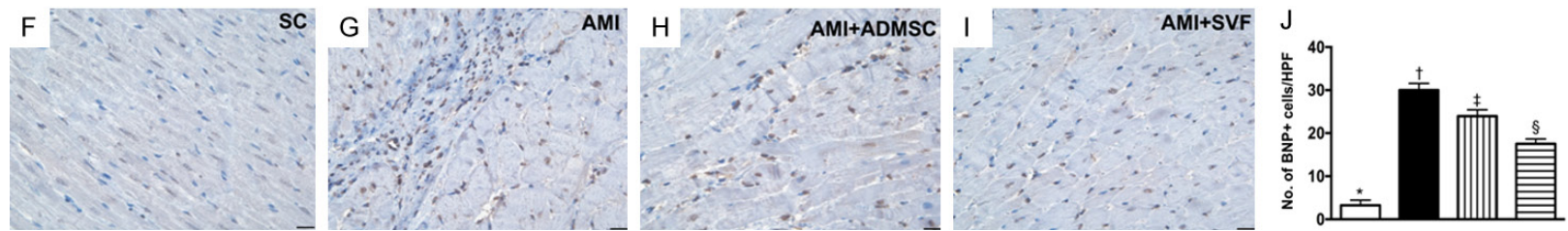
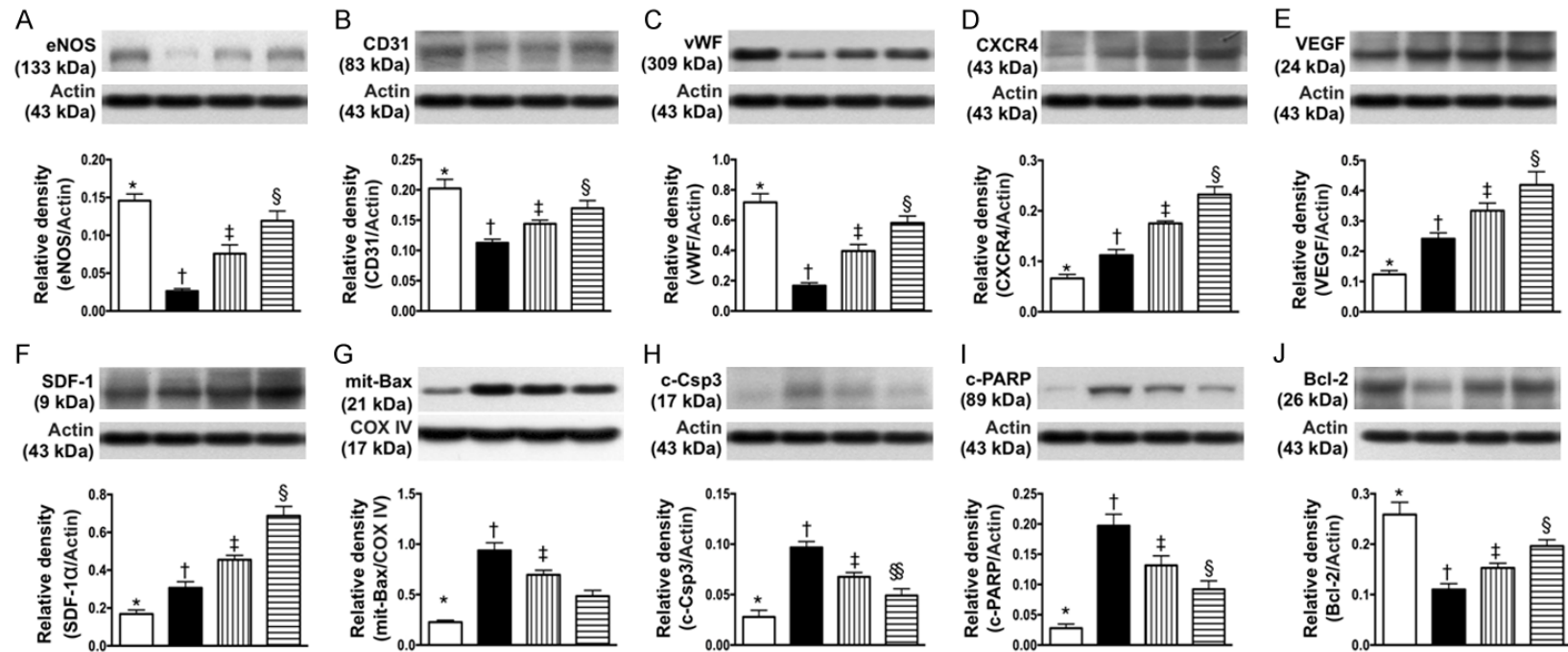


Figure 2. The microscopic findings of infarct area, fibrotic area, condensed collagen deposition area and cellular expression of heart failure biomarker in left ventricular myocardium by day 42 after AMI induction. Upper panel: A-D. Illustrating H.E. stain (100 ×) for identification of infarct area (pink-white color). a-d. Illustrating the cross section of left ventricle for identification of infarct area. E. Analytical results of the infarct area, * vs. other group with different symbols (†, ‡, §), $P < 0.0001$. F-I. Illustrating the Masson's trichrome stain (100 ×) for identification of fibrotic area (blue color). e-h. Illustrating the cross section of left ventricle for identification of fibrotic area (blue color). J. Analytical results of the infarct area, * vs. other group with different symbols (†, ‡, §), $P < 0.0001$. Lower panel: A-D. Illustrating microscopic finding (100 ×) of Sirius red stain for identification of condensed collagen-deposition area (pink color) in LV myocardium. a-d. Illustrating the cross section of left ventricle for identification of collagen-deposition area. Scale bars in right lower corner represent 100 μm. E. Analytical result of collagen-deposition area, * vs. other group with different symbols (†, ‡, §), $P < 0.0001$. F-I. Illustrating the microscopic finding (100 ×) of immunohistochemical staining for identifying the brain natriuretic peptide (BNP)-positively stained cells (gray color). Scale bars in right lower corner represent 20 μm. J. Analytical result of number of BNP+ cells, * vs. other group with different symbols (†, ‡, §), $P < 0.0001$. Symbols (*, †, ‡, §) indicate significance (at 0.05 level). SC = sham control; AMI = acute myocardial infarction; ADMSC = adipose-derived mesenchymal stem cell; SVF = stromal vascular fraction. HPF = high-power field.



SVF and ADMSC on rescuing heart function in rat after acute myocardial infarction

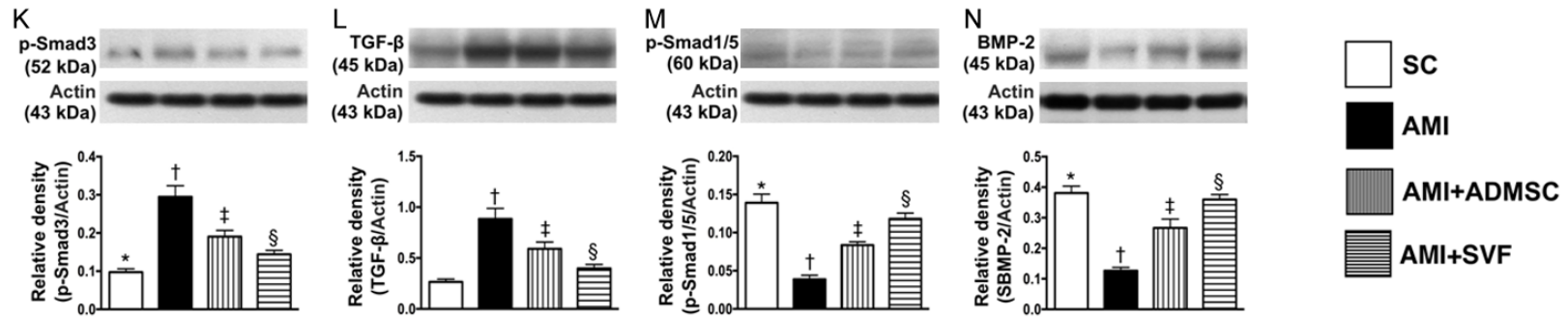


Figure 3. Protein expressions of angiogenesis, apoptotic, anti-apoptotic, fibrotic and anti-fibrotic biomarkers in left ventricular myocardium by day 42 after AMI induction. A. Protein expression of endothelial nitric oxide synthase (eNOS), * vs. other group with different symbols (†, ‡, §), $P < 0.0001$. B. Protein expression of CD31, * vs. other group with different symbols (†, ‡, §), $P < 0.001$. C. Protein expression of von Willebrand factor (vWF), * vs. other group with different symbols (†, ‡, §), $P < 0.0001$. D. Protein expression of CXCR4, * vs. other group with different symbols (†, ‡, §), $P < 0.0001$. E. Protein expression of vascular endothelial growth factor (VEGF), * vs. other group with different symbols (†, ‡, §), $P < 0.001$. F. Protein expression of stromal-cell derived factor (SDF)-1 α , * vs. other group with different symbols (†, ‡, §), $P < 0.0001$. G. Protein expression of mitochondrial (mito)-Bax, * vs. other group with different symbols (†, ‡, §), $P < 0.0001$. H. Protein expression of cleaved caspase 3 (c-Casp 3), * vs. other group with different symbols (†, ‡, §), $P < 0.0001$. I. Protein expression of cleaved poly (ADP-ribose) polymerase (PARP), * vs. other group with different symbols (†, ‡, §), $P < 0.0001$. J. Protein expression of Bcl-2, * vs. other group with different symbols (†, ‡, §), $P < 0.0001$. K. Protein phosphorylated (p)-Smad3, * vs. other group with different symbols (†, ‡, §), $P < 0.0001$. L. Protein expression of transforming growth factor (TGF)- β , * vs. other group with different symbols (†, ‡, §), $P < 0.001$. M. Protein expression of p-Smad1/5, * vs. other group with different symbols (†, ‡, §), $P < 0.0001$. N. Protein expression of bone morphogenetic protein (BMP)-2, * vs. other group with different symbols (†, ‡, §), $P < 0.0001$. SC = sham control; AMI = acute myocardial infarction; ADMSC = adipose-derived mesenchymal stem cell; SVF = stromal vascular fraction.

SVF and ADMSC on rescuing heart function in rat after acute myocardial infarction

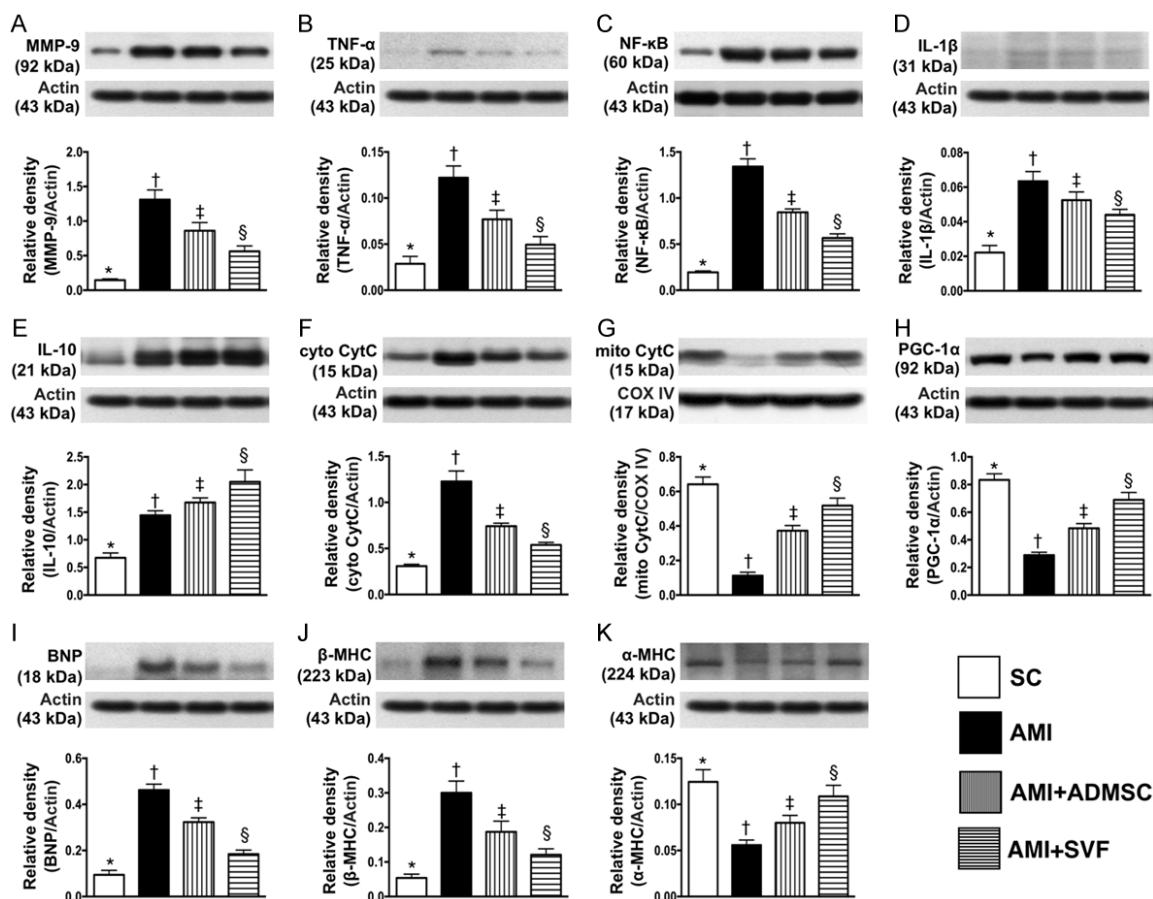


Figure 4. Protein expressions of inflammatory, mitochondrial-damaged, mitochondrial/energy-integrity and cardiac hypertrophic/heart failure biomarkers in LV myocardium by day 42 after AMI induction. A. Protein expressions of matrix metalloproteinase (MMP)-9, * vs. other group with different symbols (†, ‡, §), $P < 0.0001$. B. Protein expression of tumor necrotic factor (TNF)- α , * vs. other group with different symbols (†, ‡, §), $P < 0.0001$. C. Protein expression of nuclear factor (NF)- κ B, * vs. other group with different symbols (†, ‡, §), $P < 0.0001$. D. Protein expression of interleukin (IL)-1 β , * vs. other group with different symbols (†, ‡, §), $P < 0.001$. E. protein expression of IL-10, * vs. other group with different symbols (†, ‡, §), $P < 0.001$. F. Protein expression of cytosolic cytochrome C (cyto-Cyto C), * vs. other group with different symbols (†, ‡, §), $P < 0.001$. G. Protein expression of mitochondrial cytochrome C (mito-Cyto C), * vs. other group with different symbols (†, ‡, §), $P < 0.0001$. H. protein expression of peroxisome proliferator-activated receptor gamma coactivator-1 α (PGC-1 α), * vs. other group with different symbols (†, ‡, §), $P < 0.0001$. I. Protein expression of brain natriuretic peptide (BNP), * vs. other group with different symbols (†, ‡, §), $P < 0.0001$. J. Protein expression of β -myosin heavy chain (MHC), * vs. other group with different symbols (†, ‡, §), $P < 0.0001$. K. Protein expression of α -MHC, * vs. other group with different symbols (†, ‡, §), $P < 0.001$. SC = sham control; AMI = acute myocardial infarction; ADMSC = adipose-derived mesenchymal stem cell; SVF = stromal vascular fraction.

Protein expressions of angiogenesis, apoptotic, anti-apoptotic, fibrotic and anti-fibrotic biomarkers in LV myocardium by day 42 after AMI induction (Figure 3)

The protein expressions of endothelial nitric oxide synthase (eNOS), CD31 and von Willebrand factor (vWF), three indicators of angiogenesis, were highest in SC, lowest in AMI, and significantly higher in AMI + SVF than in AMI + ADMSC. Protein expressions of C-X-C motif chemokine receptor 4 (CXCR4), vascular

endothelial growth factor (VEGF) and stromal cell-derived factor (SDF)-1 α , another three indicators of angiogenesis, significantly and progressively increased from SC to AMI + SVF, implicating the intrinsic response to ischemic stimulation further increased after SVF/ADMS treatment.

Protein expressions of mitochondrial Bax, cleaved caspase 3 and cleaved poly(ADP-ribose) polymerase (PARP), three indicators of apoptosis, were highest in AMI, lowest in SC,

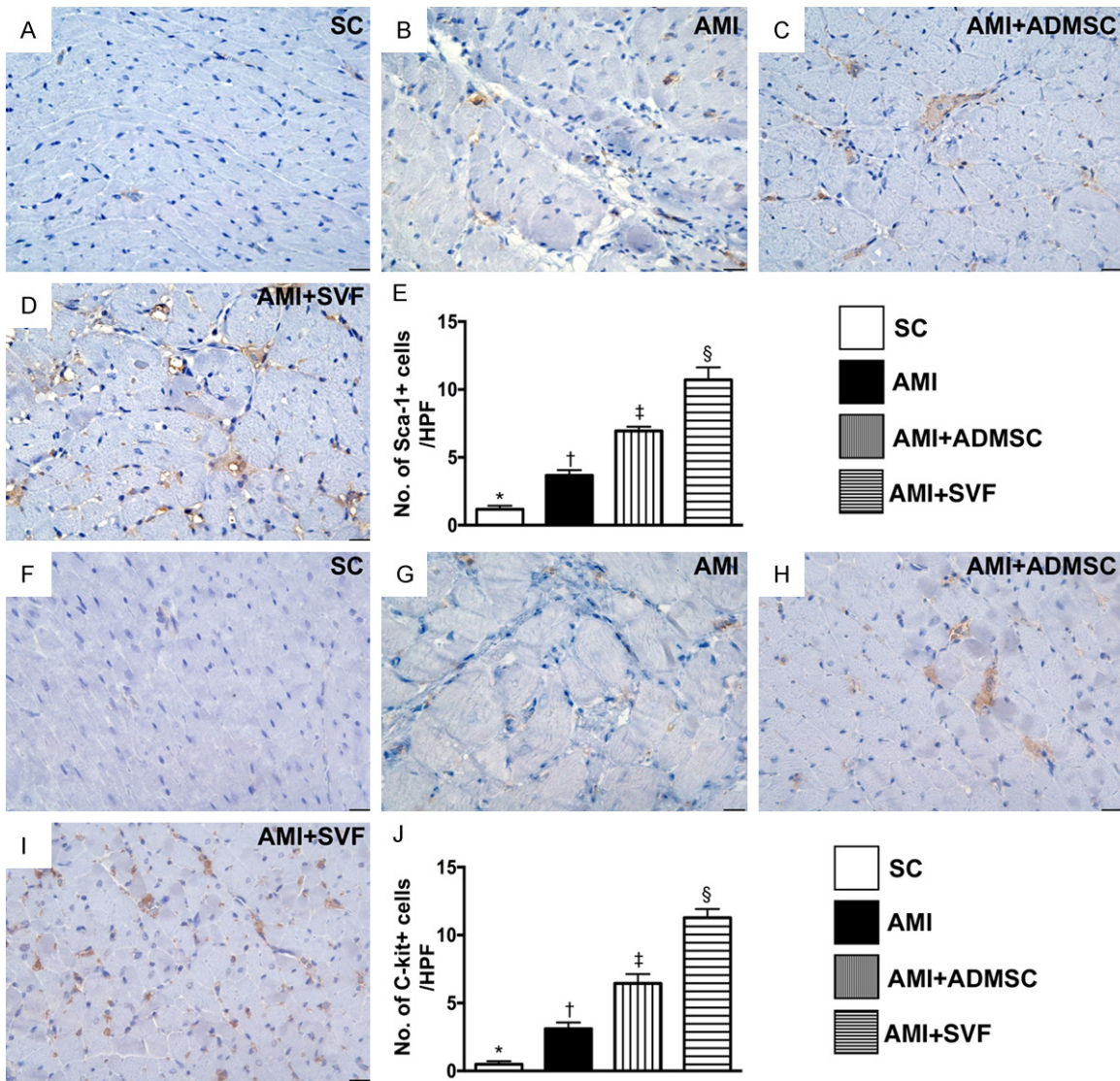


Figure 5. Cardiac stem cells in LV myocardium by day 42 after AMI induction. A-D. Illustrating immunohistochemical (IHC) microscopic finding (400 ×) for identification of Sca-1+ cells (gray color). E. Analytical results of number of Sca-1+ cells, * vs. other group with different symbols (†, ‡, §), $P < 0.0001$. F-I. Illustrating the IHC microscopic finding (400 ×) for identification of C-kit+ cells (gray color). J. Analytical results of number of C-kit+ cells, * vs. other group with different symbols (†, ‡, §), $P < 0.0001$. Scale bars in right lower corner represent 20 μm. All statistical analyses were performed by one-way ANOVA, followed by Bonferroni multiple comparison post hoc test ($n = 6$ for each group). Symbols (*, †, ‡, §) indicate significance (at 0.05 level). SC = sham control; AMI = acute myocardial infarction; ADMSC = adipose-derived mesenchymal stem cell; SVF = stromal vascular fraction. HPF = high-power field.

and significantly higher in AMI + ADMSC than in AMI + SVF. Protein expression of Bcl-2, an anti-apoptotic biomarker, demonstrated an opposite pattern to apoptosis among the four groups.

The protein expression of Smad3 and transforming growth factor (TGF)-β, two indicators of fibrosis, displayed an identical pattern to apoptosis among the four groups. The protein expressions of Smad1/5 and bone morphogenetic protein-2 (BMP-2), two indices for anti-

fibrosis, displayed an opposite pattern to fibrosis among the four groups.

Protein expressions of inflammatory, mitochondrial damaged, mitochondrial/energy-integrity and cardiac hypertrophic/heart failure in LV myocardium by day 42 after AMI induction (Figure 4)

Protein expressions of matrix metalloproteinase (MMP)-9, tumor necrosis factor (TNF)-α, nuclear factor (NF)-κB and interleukin (IL)-1β,

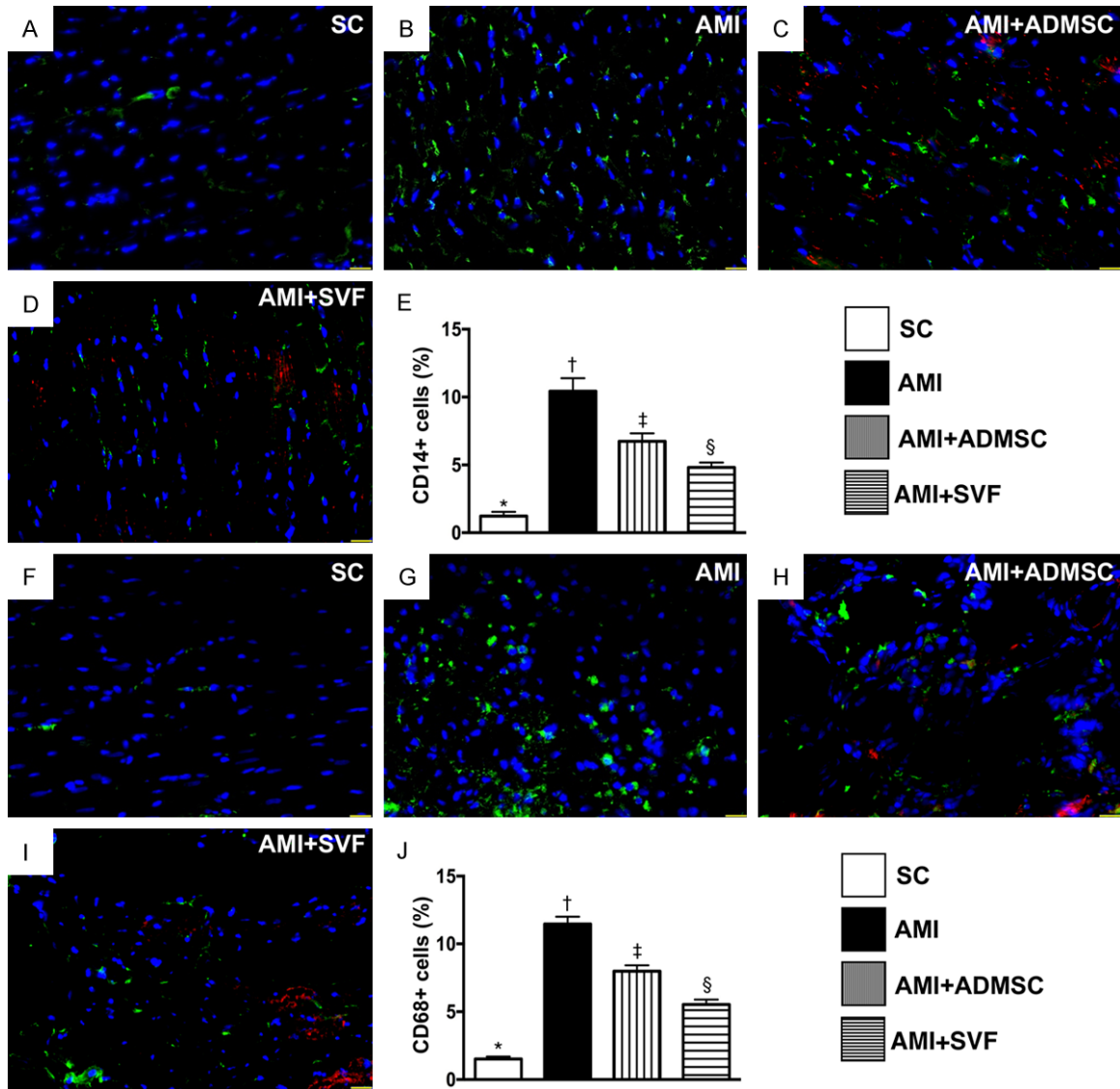


Figure 6. Inflammatory biomarkers in LV myocardium by day 42 after AMI induction. (A-D) Illustrating immunofluorescent (IF) microscopic finding (400 ×) for identification of CD14+ cells (green color). Red color in (C and D) indicated implanted ADMSC and SVF in myocardium, respectively. (E) Analytical result of percentage of CD14+ cells, * vs. other group with different symbols (†, ‡, §), $P < 0.0001$. (F-I) IF microscopic finding (400 ×) for identification of CD68+ cells (green color). Red color in (H and I) indicated implanted ADMSC and SVF in myocardium, respectively. (J) Analytical result of percentage of CD68+ cells, * vs. other group with different symbols (†, ‡, §), $P < 0.0001$. Scale bars in right lower corner represent 20 μm . All statistical analyses were performed by one-way ANOVA, followed by Bonferroni multiple comparison post hoc test ($n = 6$ for each group). Symbols (*, †, ‡, §) indicate significance (at 0.05 level). SC = sham control; AMI = acute myocardial infarction; ADMSC = adipose-derived mesenchymal stem cell; SVF = stromal vascular fraction.

four inflammatory biomarkers, were highest in AMI, lowest in SC, and significantly higher in AMI + ADMSC than in AMI + SVF. The protein expression of IL-10, an index of anti-inflammation, exhibited an opposite pattern to inflammation among the four groups.

The protein expression of cytosolic cytochrome C, an indicator of mitochondrial damage, exhib-

ited an identical pattern of inflammation among the four groups. The protein expression of mitochondrial cytochrome C, an indicator of mitochondrial integrity, displayed an opposite pattern to cytosolic cytochrome C. The protein expression of peroxisome proliferator activated receptor-gamma coactivator 1 alpha (PGC-1 α), a major upstream regulator of lipid catabolism, oxidative metabolism, mitochondrial metabo-

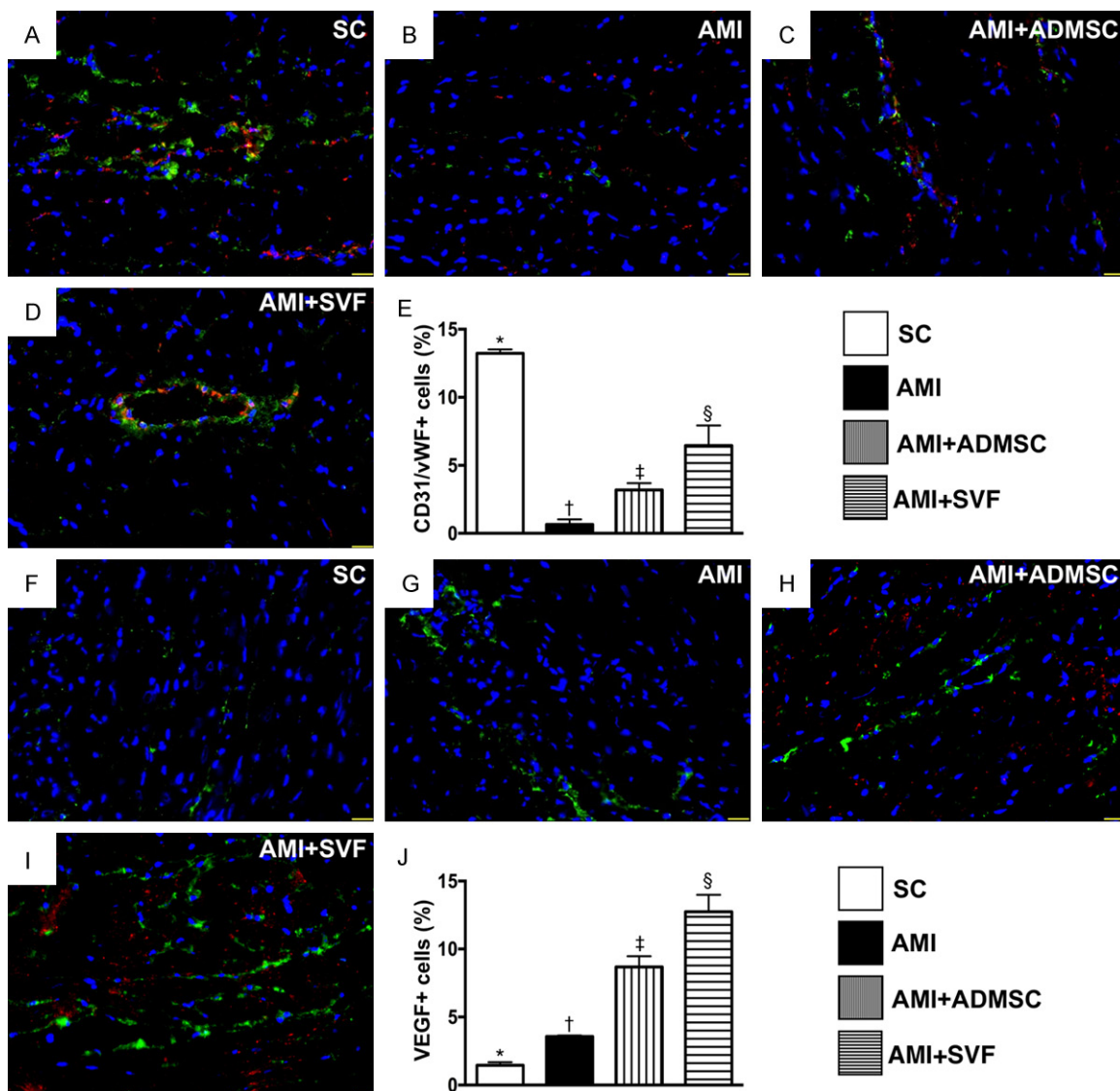


Figure 7. Cellular expression of endothelial cell biomarkers in LV myocardium by day 42 after AMI induction. (A-D) Illustrating the immunofluorescent (IF) microscopic finding (400 ×) for identification of CD31+/vov Willebran Factor (vWF)+ cells (i.e., double stain; CD31-green color; vWF-red color). (E) Analytical result of percentage of CD31+/vWF+ cells, * vs. other group with different symbols (†, ‡, §), $P < 0.0001$. (F-I) Illustrating the IF microscopic finding (400 ×) for identification of vascular endothelial growth factor (VEGF)+ cells (green color). Red color in (H and I) indicated implanted ADMSC and SVF in myocardium, respectively. (J) Analytical result of percentage of VEGF+ cells, * vs. other group with different symbols (†, ‡, §), $P < 0.0001$. Scale bars in right lower corner represent 20 μm . All statistical analyses were performed by one-way ANOVA, followed by Bonferroni multiple comparison post hoc test ($n = 6$ for each group). Symbols (*, †, ‡, §) indicate significance (at 0.05 level). SC = sham control; AMI = acute myocardial infarction; ADMSC = adipose-derived mesenchymal stem cell; SVF = stromal vascular fraction.

lism and biogenesis, showed an identical pattern to mitochondrial cytochrome C.

The protein expressions of BNP and β -myosin heavy chain (MHC), two indicators of pressure overload/heart failure, showed an identical pattern to mitochondrial cytochrome C among the four groups. Conversely, protein expression of α -MHC, a reverse myocardial hypertrophic

biomarker, showed an opposite pattern to β -MHC among the four groups.

Cardiac stem cell and inflammatory biomarkers in LV myocardium by day 42 after AMI induction (Figures 5 and 6)

IHC microscopy showed that the number of C-kit+ and Sca-1+ cells, two cardiac stem cell

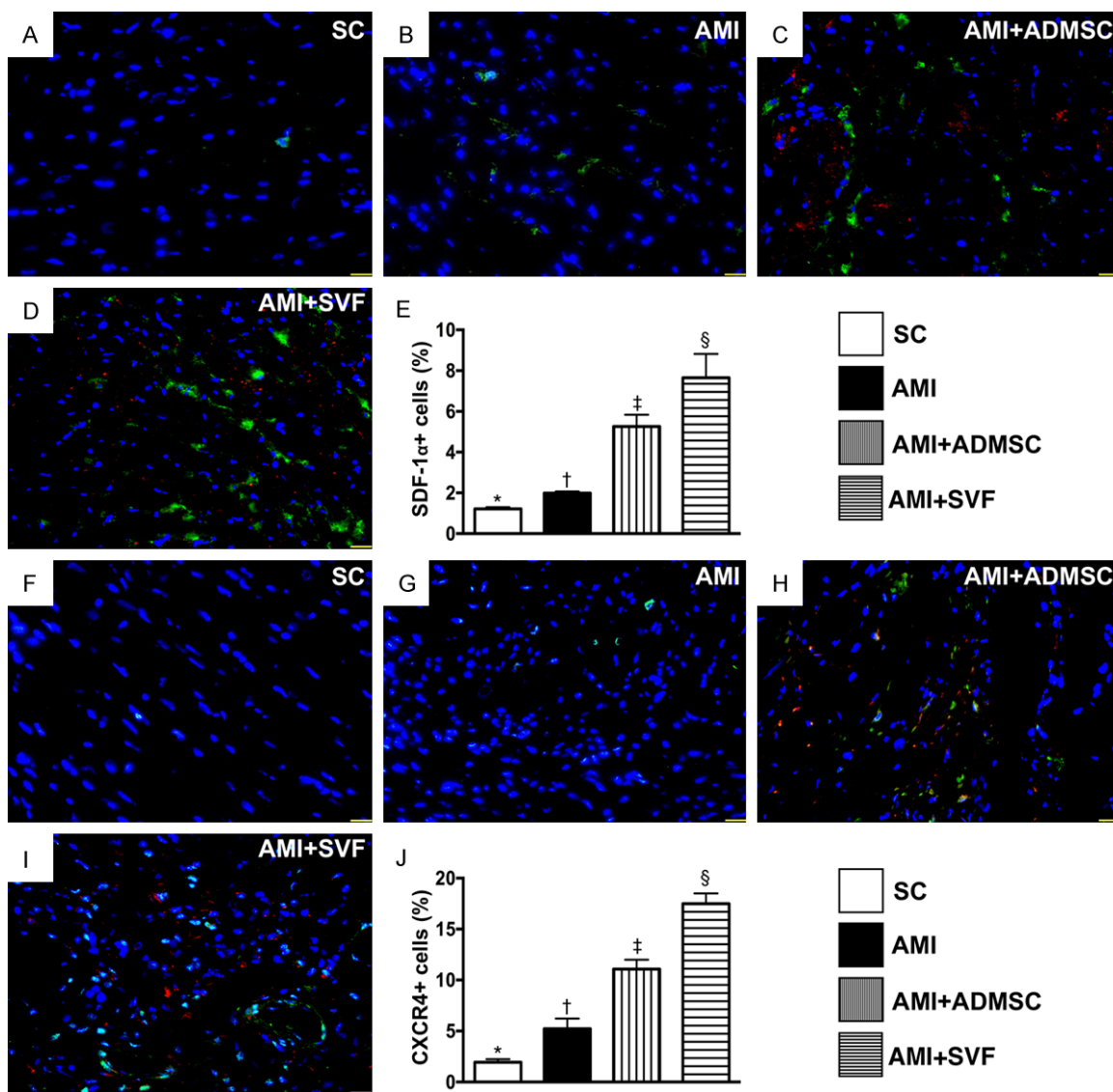


Figure 8. Cellular expressions of endothelial progenitor cell (EPC) biomarkers in LV myocardium by day 42 after AMI induction. (A-D) Illustrating the immunofluorescent (IF) microscopic finding (400 ×) for identification of stromal-cell derived factor (SDF)-1α+ cells (green color). Red color in (C and D) indicated implanted ADMSC and SVF in myocardium, respectively. (E) Analytical result of percentage of SDF-1α+ cells, * vs. other group with different symbols (†, ‡, §), $P < 0.0001$. (F-I) Illustrating the IF microscopic finding (400 ×) for identification of CXCR4+ cells (green color). Red color in (H and I) indicated implanted ADMSC and SVF in myocardium, respectively. (J) Analytical result of percentage of CXCR4+ cells, * vs. other group with different symbols (†, ‡, §), $P < 0.0001$. Scale bars in right lower corner represent 20 μm. All statistical analyses were performed by one-way ANOVA, followed by Bonferroni multiple comparison post hoc test ($n = 6$ for each group). Symbols (*, †, ‡, §) indicate significance (at 0.05 level). SC = sham control; AMI = acute myocardial infarction; ADMSC = adipose-derived mesenchymal stem cell; SVF = stromal vascular fraction.

indicators (Figure 5), significantly and progressively increased from SC to AMI + SVF, suggesting an intrinsic response to ischemic stimulation, and increased further after SVF/ADMS treatment.

Immunofluorescence (IF) microscopy demonstrated that the number of CD14+ and CD68+ cells, two indicators of inflammation, were high-

est in AMI, lowest in SC and significantly higher in AMI + ADMSC than in AMI + SVF (Figure 6).

The cellular expression of endothelial cell biomarkers in LV myocardium by day 42 after AMI induction (Figure 7)

IF microscopy identified that the number of CD31+/vWF+ cells (i.e., double stained), an EC

SVF and ADMSC on rescuing heart function in rat after acute myocardial infarction

biomarker, was highest in SC, lowest in AMI, and significantly higher in AMI + SVF than in AMI + ADMSC. IF microscopy also demonstrated that the number of VEGF+ cells, another EC biomarker, significantly and progressively increased from SC to AMI + SVF.

The cellular expressions of EPC biomarkers in LV myocardium by day 42 after AMI induction (Figure 8)

IF microscopy demonstrated that the numbers of SDF-1 α + and CXCR4+ cells, two EPC biomarkers, significantly and progressively increased from SC to AMI + SVF.

The cellular expressions of DNA damaged and gap junction biomarkers in LV myocardium by day 42 after AMI induction (Figure 9)

IF microscopy showed that the number of phosphorylated histone H2AX (γ -H2AX), an indicator of DNA-damage, was highest in AMI, lowest in SC, and significantly higher in AMI + ADMSC than in AMI + SVF. IF microscopy also exhibited that the area of positively-stained connexin43 (Cx43), an indicator of gap junction for cellular interaction/communication, was highest in SC, lowest in AMI, and significantly higher in AMI + SVF than in AMI + ADMSC.

Discussion

This study investigated the potential therapeutic effect of SVF and ADMSC on improving LV function and inhibiting LV remodeling in rat after AMI and yielded several striking implications. First, the therapeutic effect of SVF was superior, rather than non-inferior, to ADMSC for improving LVEF and attenuating LV remodeling. Second, areas of infarction, fibrosis and collagen deposition in LV myocardium were remarkably reduced in the SVF group compared to the ADMSC group, implicating that the therapeutic benefit of SVF was better than ADMSC in the setting of AMI. Third, angiogenesis was found to be one of the paramount factors for preserving heart function and architecture of LV myocardium.

Experimental studies and clinical trials have shown that cell therapy shows promise in improving ischemia-related LV dysfunction [11-19]. An essential finding in the present study was that LVEF (i.e., functional assessment) was improved and LV remodeling (i.e., structural

assessment) was inhibited in AMI animals with ADMSC treatment compared to AMI animals without treatment, which is consistent with previous studies [11-19]. While the therapeutic impact of SVF on wound healing has been keenly investigated [20-23], the therapeutic impact of SVF on AMI has seldom been reported and, importantly, the result was uncertain [24]. The most important finding in the present study was that LVEF was further improved and LV remodeling was further suppressed in SVF-treated animals compared to ADMSC-treated animals, suggesting that SVF may be more effective than ADMSC at improving prognosis after AMI. Our findings, therefore, extend those of previous work [24], and encouraged our design of a prospective study looking at SVF as a possible accessory treatment for AMI patients after receiving primary PCI treatment.

A principal finding in the present study was that the anatomical-histopathological studies (i.e., structural assessment) showed that infarction, fibrosis and collagen-deposition areas were substantially increased in the AMI group than controls. These parameters were markedly reduced in AMI animals after receiving ADMSC treatment. Previous studies have shown that MSC, including ADMSC therapy, significantly reduced infarct area and preserved LV function and hence the present study corroborates those previous studies [24, 25, 31]. SVF therapy offered an additional benefit over ADMSC on reducing infarction, fibrosis and collagen-deposition areas, hence LVEF was more preserved and LV remodeling was further inhibited in SVF-treated than ADMSC-treated animals.

The mechanisms underlying how MSC treatment might lead to improved heart function after AMI has been intensively discussed and is considered multifactorial, involving angiogenesis, paracrine/chemokine effects, stem cell homing, and implanted MSC differentiation into and integration with cardiomyocytes [12, 15, 24, 25, 31]. Of these, angiogenesis has been established as one of the most important factors for restoring blood flow and tissue/organ regeneration [12, 15, 24, 25, 31]. One important finding in the present study was that the flow cytometric and qPCR (i.e., *in vitro* study) analyses showed that the cellular and gene expressions of EPC (i.e., angiogenesis markers) and Sca-1/C-kit (i.e., cardiac stem cell) bio-

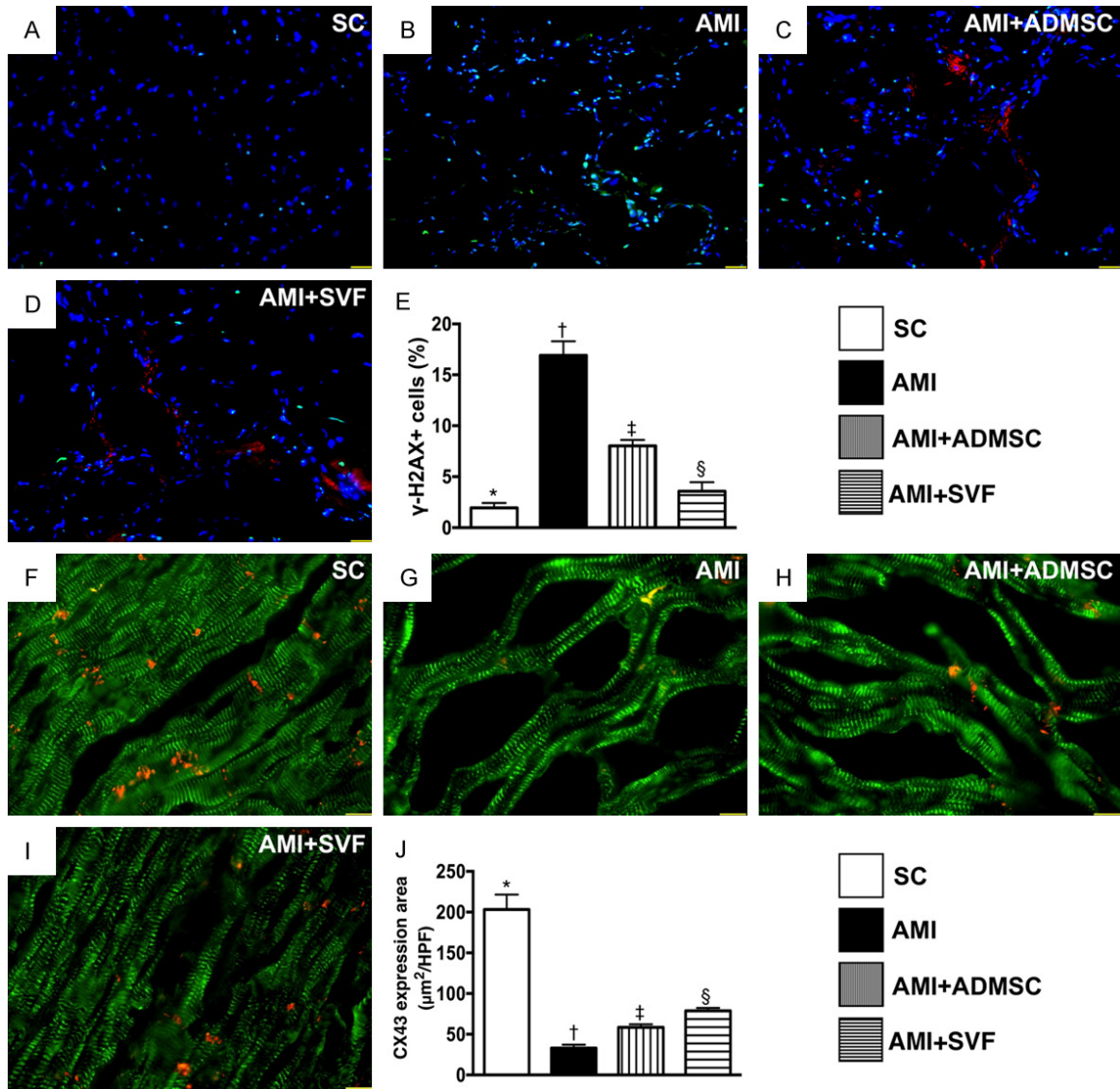


Figure 9. Cellular expressions of DNA-damaged and gap-junction biomarkers in LV myocardium by day 42 after AMI induction. A-D. Illustrating the immunofluorescent (IF) microscopic finding (400 ×) for identification of γ -H2AX+ cells (pink color). Scale bars in right lower corner represent 20 μ m. E. Analytical result of percentage of γ -H2AX+ cells, * vs. other group with different symbols (†, ‡, §), $P < 0.0001$. F-I. Illustrating IF microscopic finding (1000 ×) for identification of distributive area of positively-stained CX43 (red color). J. Analytical result of Cx43 expression area per high-power field (HPF), * vs. other group with different symbols (†, ‡, §), $P < 0.0001$. All statistical analyses were performed by one-way ANOVA, followed by Bonferroni multiple comparison post hoc test ($n = 6$ for each group). Symbols (*, †, ‡, §) indicate significance (at 0.05 level). SC = sham control; AMI = acute myocardial infarction; ADMSC = adipose-derived mesenchymal stem cell; SVF = stromal vascular fraction. HPF = high-power field.

markers were significantly higher in SVF group than in ADMSC group. Our findings highlighted that angiogenesis capacity was higher in SVF than in ADMSC. Another important finding was that the protein and cellular expression of angiogenesis biomarkers and number of small vessels in heart specimens were notably increased in ADMSC-treated and further increased in SVF-treated animals compared to

AMI only animals. Accordingly, our in vitro results supported the findings from the in vivo studies. Furthermore, our in vivo results, in addition to supporting the findings of previous studies [12, 15, 24, 25, 31], could, at least in part, explain why LVEF was significantly increased and LV remodeling/infarct size were significantly suppressed in SVF-treated animals compared to ADMSC-treated animals.

Associations between reduced heart function and increased inflammatory reaction, apoptosis, fibrosis, and DNA/mitochondrial damage have all been well recognized in the AMI setting [12, 15, 24, 25, 31]. An important finding in the present study was that, compared to the sham control group, these aforementioned biomarkers were substantially increased in AMI animals, markedly reduced in ADMSC-treated animals and further reduced in SVF-treated animals. These findings, in addition to supporting previous studies [12, 15, 24, 25, 31], could once again explain why SVF is superior to ADMSC for preserving heart function in animals after AMI.

Links between increases in pressure-overload/heart failure biomarkers and decreases in CX43 expression (i.e., gap junction for cell to cell interaction and communication) as well as arterial muscularization and poorer LV function in AMI have been keenly investigated [12, 15, 24, 25, 31]. An intriguing finding in the present study was that pressure-overload/heart failure, cardiac hypertrophy biomarkers and vessel muscularization were significantly increased, whilst CX43 expression on LV myocardium was notably reduced, in AMI animals compared to controls, and these were reversed in ADMSC-treated and more significantly reversed in SVF-treated animals. Our findings therefore reinforce previous studies [12, 15, 24, 25, 31] and provide some explanation for the superior benefit of SVF over ADMSC on improving LV function.

Acknowledgements

This study was supported by a program grant from Chang Gung Memorial Hospital, Chang Gung University (Grant number: CMRPG8E-0671). We thank the molecular imaging core of the Center for Translational Research in Biomedical Sciences, Kaohsiung Chang Gung Memorial Hospital, Kaohsiung, Taiwan for technical and facility supports on Echo Vevo 2100.

Disclosure of conflict of interest

None.

Abbreviations

AMI, acute myocardial infarction; ADMSC, adipose-derived mesenchymal stem cell; BMP, bone morphogenetic protein; EPC, endothelial

progenitor cells; IL, interleukin; LVEF, left ventricular ejection fraction; LVEDd, left ventricular end-diastolic dimension; LVESd, left ventricular end-systolic dimension; MMP, matrix metalloproteinase; MSC, mesenchymal stem cell; MHC, myosin heavy chain; NF, nuclear factor; SDF, stromal cell-derived factor; SVF, stromal vascular fraction; TGF, transforming growth factor; TNF, tumor necrosis factor; vWF, Willebrand factor; VEGF, vascular endothelial growth factor.

Address correspondence to: Jiunn-Jye Sheu, Division of Thoracic and Cardiovascular Surgery, Department of Surgery, Kaohsiung Chang Gung Memorial Hospital and Chang Gung University College of Medicine, Kaohsiung 83301, Taiwan. E-mail: cvsjs@gmail.com; Hon-Kan Yip, Division of Cardiology, Department of Internal Medicine, Kaohsiung Chang Gung Memorial Hospital and Chang Gung University College of Medicine, Kaohsiung 83301, Taiwan. E-mail: han.gung@msa.hinet.net

References

- [1] Sheu JJ, Tsai TH, Lee FY, Fang HY, Sun CK, Leu S, Yang CH, Chen SM, Hang CL, Hsieh YK, Chen CJ, Wu CJ and Yip HK. Early extracorporeal membrane oxygenator-assisted primary percutaneous coronary intervention improved 30-day clinical outcomes in patients with ST-segment elevation myocardial infarction complicated with profound cardiogenic shock. *Crit Care Med* 2010; 38: 1810-1817.
- [2] Ahmad Y, Sen S, Shun-Shin MJ, Ouyang J, Finegold JA, Al-Lamee RK, Davies JE, Cole GD and Francis DP. Intra-aortic balloon pump therapy for acute myocardial infarction: a meta-analysis. *JAMA Intern Med* 2015; 175: 931-939.
- [3] Su D, Yan B, Guo L, Peng L, Wang X, Zeng L, Ong H and Wang G. Intra-aortic balloon pump may grant no benefit to improve the mortality of patients with acute myocardial infarction in short and long term: an updated meta-analysis. *Medicine (Baltimore)* 2015; 94: e876.
- [4] Chung SY, Tong MS, Sheu JJ, Lee FY, Sung PH, Chen CJ, Yang CH, Wu CJ and Yip HK. Short-term and long-term prognostic outcomes of patients with ST-segment elevation myocardial infarction complicated by profound cardiogenic shock undergoing early extracorporeal membrane oxygenator-assisted primary percutaneous coronary intervention. *Int J Cardiol* 2016; 223: 412-417.
- [5] Ouweneel DM, Eriksen E, Sjauw KD, van Dongen IM, Hirsch A, Packer EJ, Vis MM, Wykrzykowska JJ, Koch KT, Baan J, de Winter RJ, Piek JJ, Lagrand WK, de Mol BA, Tijssen JG

- and Henriques JP. Percutaneous mechanical circulatory support versus intra-aortic balloon pump in cardiogenic shock after acute myocardial infarction. *J Am Coll Cardiol* 2017; 69: 278-287.
- [6] Kawaji T, Shiomi H, Morimoto T, Furukawa Y, Nakagawa Y, Kadota K, Ando K, Mizoguchi T, Abe M, Takahashi M, Kimura T; CREDO-Kyoto AMI investigators. Long-term clinical outcomes in patients with ST-segment elevation acute myocardial infarction complicated by cardiogenic shock due to acute pump failure. *Eur Heart J Acute Cardiovasc Care* 2018; 7: 743-754.
- [7] Kim TH, Lee KY, Choi Y, Park HW, Lee YS, Koh YS, Park HJ, Kim PJ, Chang K, Chung WS, Kim DB, Her SH, Park CS, Lee JM, Kim HY, Yoo KD, Jeon DS, Ahn Y, Jeong MH and Seung KB. Prognostic importance of mitral regurgitation complicated by acute myocardial infarction during a 5-year follow-up period in the drug-eluting stent era. *Coron Artery Dis* 2016; 27: 109-115.
- [8] Gyongyosi M, Giurgea GA, Syeda B, Charwat S, Marzluf B, Mascherbauer J, Jakab A, Zimba A, Sarkozy M, Pavo N, Sochor H, Graf S, Lang I, Maurer G, Bergler-Klein J and investigators M. Long-term outcome of combined (Percutaneous Intramyocardial and Intracoronary) application of autologous bone marrow mononuclear cells post myocardial infarction: the 5-Year MYSTAR study. *PLoS One* 2016; 11: e0164908.
- [9] Taniguchi T, Shiomi H, Morimoto T, Watanabe H, Ono K, Shizuta S, Kato T, Saito N, Kaji S, Ando K, Kadota K, Furukawa Y, Nakagawa Y, Horie M and Kimura T. Incidence and prognostic impact of heart failure hospitalization during follow-up after primary percutaneous coronary intervention in ST-segment elevation myocardial infarction. *Am J Cardiol* 2017; 119: 1729-1739.
- [10] Winter MP, Blessberger H, Alimohammadi A, Pavo N, Huber K, Wojta J, Lang IM, Wiesbauer F and Gollasch G. Long-term outcome and risk assessment in premature acute myocardial infarction: a 10-year follow-up study. *Int J Cardiol* 2017; 240: 37-42.
- [11] Nanjundappa A, Raza JA, Dieter RS, Mandapaka S and Cascio WE. Cell transplantation for treatment of left-ventricular dysfunction due to ischemic heart failure: from bench to bedside. *Expert Rev Cardiovasc Ther* 2007; 5: 125-131.
- [12] Leu S, Sun CK, Sheu JJ, Chang LT, Yuen CM, Yen CH, Chiang CH, Ko SF, Pei SN, Chua S, Youssef AA, Wu CJ and Yip HK. Autologous bone marrow cell implantation attenuates left ventricular remodeling and improves heart function in porcine myocardial infarction: an echocardiographic, six-month angiographic, and molecular-cellular study. *Int J Cardiol* 2011; 150: 156-168.
- [13] Zimmet H, Porapakham P, Porapakham P, Sata Y, Haas SJ, Itescu S, Forbes A and Krum H. Short- and long-term outcomes of intracoronary and endogenously mobilized bone marrow stem cells in the treatment of ST-segment elevation myocardial infarction: a meta-analysis of randomized control trials. *Eur J Heart Fail* 2012; 14: 91-105.
- [14] Lee FY, Chen YL, Sung PH, Ma MC, Pei SN, Wu CJ, Yang CH, Fu M, Ko SF, Leu S and Yip HK. Intracoronary transfusion of circulation-derived CD34+ cells improves left ventricular function in patients with end-stage diffuse coronary artery disease unsuitable for coronary intervention. *Crit Care Med* 2015; 43: 2117-2132.
- [15] Sheu JJ, Lee FY, Yuen CM, Chen YL, Huang TH, Chua S, Chen YL, Chen CH, Chai HT, Sung PH, Chang HW, Sun CK and Yip HK. Combined therapy with shock wave and autologous bone marrow-derived mesenchymal stem cells alleviates left ventricular dysfunction and remodeling through inhibiting inflammatory stimuli, oxidative stress & enhancing angiogenesis in a swine myocardial infarction model. *Int J Cardiol* 2015; 193: 69-83.
- [16] Quyyumi AA, Vasquez A, Kereiakes DJ, Klapholz M, Schaer GL, Abdel-Latif A, Frohwein S, Henry TD, Schatz RA, Dib N, Toma C, Davidson CJ, Barsness GW, Shavelle DM, Cohen M, Poole J, Moss T, Hyde P, Kanakaraj AM, Druker V, Chung A, Junge C, Preti RA, Smith RL, Mazzo DJ, Pecora A and Losordo DW. PreSERVE-AMI: a randomized, double-blind, placebo-controlled clinical trial of intracoronary administration of autologous CD34+ cells in patients with left ventricular dysfunction post STEMI. *Circ Res* 2017; 120: 324-331.
- [17] Banas A, Teratani T, Yamamoto Y, Tokuhara M, Takeshita F, Osaki M, Kawamata M, Kato T, Okochi H and Ochiya T. IFATS collection: in vivo therapeutic potential of human adipose tissue mesenchymal stem cells after transplantation into mice with liver injury. *Stem Cells* 2008; 26: 2705-2712.
- [18] Leu S, Lin YC, Yuen CM, Yen CH, Kao YH, Sun CK and Yip HK. Adipose-derived mesenchymal stem cells markedly attenuate brain infarct size and improve neurological function in rats. *J Transl Med* 2010; 8: 63.
- [19] Chen YT, Sun CK, Lin YC, Chang LT, Chen YL, Tsai TH, Chung SY, Chua S, Kao YH, Yen CH, Shao PL, Chang KC, Leu S and Yip HK. Adipose-derived mesenchymal stem cell protects kidneys against ischemia-reperfusion injury through suppressing oxidative stress and inflammatory reaction. *J Transl Med* 2011; 9: 51.
- [20] Casteilla L, Planat-Benard V, Laharrague P and Cousin B. Adipose-derived stromal cells: their identity and uses in clinical trials, an update. *World J Stem Cells* 2011; 3: 25-33.

SVF and ADMSC on rescuing heart function in rat after acute myocardial infarction

- [21] Kern S, Eichler H, Stoeve J, Kluter H and Bieback K. Comparative analysis of mesenchymal stem cells from bone marrow, umbilical cord blood, or adipose tissue. *Stem Cells* 2006; 24: 1294-1301.
- [22] Gimble JM, Bunnell BA, Chiu ES and Guilak F. Concise review: adipose-derived stromal vascular fraction cells and stem cells: let's not get lost in translation. *Stem Cells* 2011; 29: 749-754.
- [23] Atalay S, Coruh A and Deniz K. Stromal vascular fraction improves deep partial thickness burn wound healing. *Burns* 2014; 40: 1375-1383.
- [24] van Dijk A, Naaijken BA, Jurgens WJ, Nalliah K, Sairras S, van der Pijl RJ, Vo K, Vonk AB, van Rossum AC, Paulus WJ, van Milligen FJ and Niessen HW. Reduction of infarct size by intravenous injection of uncultured adipose derived stromal cells in a rat model is dependent on the time point of application. *Stem Cell Res* 2011; 7: 219-229.
- [25] Yip HK, Chang LT, Wu CJ, Sheu JJ, Youssef AA, Pei SN, Lee FY and Sun CK. Autologous bone marrow-derived mononuclear cell therapy prevents the damage of viable myocardium and improves rat heart function following acute anterior myocardial infarction. *Circ J* 2008; 72: 1336-1345.
- [26] Sun CK, Zhen YY, Leu S, Tsai TH, Chang LT, Sheu JJ, Chen YL, Chua S, Chai HT, Lu HI, Chang HW, Lee FY and Yip HK. Direct implantation versus platelet-rich fibrin-embedded adipose-derived mesenchymal stem cells in treating rat acute myocardial infarction. *Int J Cardiol* 2014; 173: 410-423.
- [27] Aird AL, Nevitt CD, Christian K, Williams SK, Hoying JB and LeBlanc AJ. Adipose-derived stromal vascular fraction cells isolated from old animals exhibit reduced capacity to support the formation of microvascular networks. *Exp Gerontol* 2015; 63: 18-26.
- [28] Chen HH, Lin KC, Wallace CG, Chen YT, Yang CC, Leu S, Chen YC, Sun CK, Tsai TH, Chen YL, Chung SY, Chang CL and Yip HK. Additional benefit of combined therapy with melatonin and apoptotic adipose-derived mesenchymal stem cell against sepsis-induced kidney injury. *J Pineal Res* 2014; 57: 16-32.
- [29] Lin KC, Yip HK, Shao PL, Wu SC, Chen KH, Chen YT, Yang CC, Sun CK, Kao GS, Chen SY, Chai HT, Chang CL, Chen CH and Lee MS. Combination of adipose-derived mesenchymal stem cells (ADMSC) and ADMSC-derived exosomes for protecting kidney from acute ischemia-reperfusion injury. *Int J Cardiol* 2016; 216: 173-185.
- [30] Sung PH, Chiang HJ, Chen CH, Chen YL, Huang TH, Zhen YY, Chang MW, Liu CF, Chung SY, Chen YL, Chai HT, Sun CK and Yip HK. Combined therapy with adipose-derived mesenchymal stem cells and ciprofloxacin against acute urogenital organ damage in rat sepsis syndrome induced by intrapelvic injection of cecal bacteria. *Stem Cells Transl Med* 2016; 5: 782-792.
- [31] Chua S, Lee FY, Chiang HJ, Chen KH, Lu HI, Chen YT, Yang CC, Lin KC, Chen YL, Kao GS, Chen CH, Chang HW and Yip HK. The cardioprotective effect of melatonin and exendin-4 treatment in a rat model of cardiorenal syndrome. *J Pineal Res* 2016; 61: 438-456.
- [32] Chen YL, Sun CK, Tsai TH, Chang LT, Leu S, Zhen YY, Sheu JJ, Chua S, Yeh KH, Lu HI, Chang HW, Lee FY and Yip HK. Adipose-derived mesenchymal stem cells embedded in platelet-rich fibrin scaffolds promote angiogenesis, preserve heart function, and reduce left ventricular remodeling in rat acute myocardial infarction. *Am J Transl Res* 2015; 7: 781-803.
- [33] Chen HH, Chen YT, Yang CC, Chen KH, Sung PH, Chiang HJ, Chen CH, Chua S, Chung SY, Chen YL, Huang TH, Kao GS, Chen SY, Lee MS and Yip HK. Melatonin pretreatment enhances the therapeutic effects of exogenous mitochondria against hepatic ischemia-reperfusion injury in rats through suppression of mitochondrial permeability transition. *J Pineal Res* 2016; 61: 52-68.